INSTITUTE FOR FUSION STUDIES

DOE/ET-53088-553 IFSR #553

Anomalous Ion Thermal Transport in Hot Ion Plasmas by the Ion Temperature Gradient Mode

J.Y. KIM, W. HORTON
Institute for Fusion Studies
The University of Texas at Austin
Austin, Texas 78712
and
B. COPPI
Research Laboratory of Electronics
Massachusetts Institute of Technology
Cambridge, Massachusetts 02139

June 1992

THE UNIVERSITY OF TEXAS

AUSTIN

Anomalous Ion Thermal Transport in Hot Ion Plasmas by the Ion Temperature Gradient Mode

J.Y. KIM and W. HORTON
Institute for Fusion Studies
The University of Texas at Austin
Austin, Texas 78712
and
B. COPPI
Research Laboratory of Electronics
Massachusetts Institute of Technology
Cambridge, Massachusetts 02139

Abstract

Experiments show that the observed radial profiles of the ion thermal conductivity χ_i have the opposite shapes with those obtained from the ion temperature gradient mode (η_i mode) turbulence model by the traditional mixing length estimate. In this work, this radial profile problem is reconsidered with an electromagnetic study of the linear stability of the toroidal η_i mode and a new rule for choosing the mixing length. It is first shown that the electromagnetic effect gives a significant stabilizing effect on the toroidal η_i mode, and that the observed reduction of $\chi_i(r)$ in the core region can be explained by this electromagnetic effect. Secondly, in view of earlier numerical simulations showing the transfer of fluctuation energy to larger scales than those for the fastest growth rate, as well as fluctuation measurements indicating longer radial correlation lengths, a new mixing length formula is proposed to explain the radial

increase of the χ_i. It is shown that the new formula fits well the observed $\chi_i(r)$ profiles in two TFTR supershot discharges and also gives the scaling law in the current and the magnetic field which agrees better with experiment than the conventional formula.

In controlled fusion research, the anomalous transport of the particle and energy is one of the most important problems to overcome. It is generally believed that this anomalous transport occurs by various microinstabilities, such as the ion temperature gradient mode (so-called η_i mode), the trapped electron and ion modes, and the resistive magnetohydrodynamic modes. Among these instabilities, the η_i mode is recognized as a main cause of the anomalous thermal transport for the ion component. Recently, several experimental attempts[1,2] have been carried out to test more directly the hypothesis that the anomalous ion transport is due to the η_i mode. In these experiments, the ion thermal conductivity χ_i has been measured as a function of radius and compared roughly with some theoretical models[3,4] of the η_i mode. In relation to these experiments, Horton *et al.*[5] performed a more detailed comparison of the experimental results of the TFTR 44669 supershot discharge with various theoretical models of the η_i mode. One of main problems commonly found from these comparisons is that it is difficult to explain theoretically the observed radial increase of $\chi_i(r)$.

To obtain some understanding of this radial profile problem we reconsider the simple mixing length formula which is used to calculate χ_i in most theoretical studies. In these studies, the mixing length formula assumes that in the turbulent state the dominant transport occurs by the mode with the maximum growth rate $\gamma_{\max}$ with the scale length of the mixing determined by the same mode. Thus, the mixing length formula takes the following simple form $\gamma_{\max}/k_{\perp,\max}^2$, where $k_{\perp,\max}^{-1}$ is the radial width of the mode with the maximum growth rate $\gamma_{\max}$. Here, the isotropic approximation $k_\perp \simeq k_y$ is usually taken, based on the fact that the numerical simulation results[6,7,8] show that in the turbulent state the fluctuations take on approximately the isotropic structure. Also, since the kinetic studies[9,10] of the linear stability of the toroidal η_i mode show that the maximum growth rate occurs about at $k_y\rho_i \simeq 0.5$ over a wide range of parameters, the mixing length formula leads to the thermal

diffusivity given approximately by

$$\chi_i \simeq 4\gamma_{\max}\rho_i^2. \tag{1}$$

Now, noting that the growth rate γ scales nearly as $\gamma \propto v_i$ for constant T_i/T_e, we can see that $\chi_i \propto T_i^{3/2}$. Thus, the theoretical χ_i from the simple mixing length argument produces the χ_i profile which decreases radially like the temperature profile — opposite to the experimental diffusivity.

This profile problem encountered in the theoretical modeling using the simple mixing length formula may be separated into the following two questions. First, why is the actual transport in the core region with the high ion temperature much smaller than that expected. Secondly, why does the actual transport increase with the minor radius. Of course, these two questions may be closely related. In this work, we try to answer these two questions through the more complete study of the toroidal η_i mode.

First, we consider the first question about the χ_i's decrease in the core region. A plausible explanation of this question is that the η_i modes become stable in the core region by some stabilizing effects. One such stabilizing factor is the parallel ion transit drift effect. In Fig. 1, we show the result of three standard mixing length models for the TFTR 44669A supershot discharge (a detailed overview of the TFTR 44669A discharge can be found in Ref. 5). Figure 1 shows clearly that if we take $k_{||} = 1/Rq$ the decrease of the χ_i in the core region ($r < 0.3m$) can be explained in agreement with the experiment. However, the more exact nonlocal result, which was obtained by solving the gyrokinetic equation[3,10] in the ballooning space, shows that the local assumption $k_{||} = 1/Rq$ overestimates significantly the actual effect of the parallel ion transit term. The nonlocal analysis shows that the actual value of $k_{||}$ is about $1/2Rq$ less than $1/Rq$, and this value is too small to give the decrease of the χ_i in the core region. The rapid vanishing of the mixing length χ_i's in Fig. 1 in the deep center region of $r < 0.1m$ is found by parametric variation to come mainly from the stabilizing effect[3,11] of the adiabatic electron term $\tau = T_i/T_e$. However, this $\tau = T_i/T_e$

effect is still ineffective to reduce the χ_i in the intermediate core region of $0.1m < r < 0.3m$. Furthermore, this τ effect is significant only for the hot ion temperature plasma such as in the supershot discharge analyzed here, and can not explain the decrease of χ_i in discharges with $T_i \simeq T_e$. Thus, the analysis shows that neither the parallel transit drift nor the $\tau = T_i/T_e$ stabilization can explain sufficiently the decrease of the χ_i in the core region. Now, we consider the electromagnetic effect as another core stabilizing factor.

There are many previous works[12-15] which studied the electromagnetic effect on the toroidal η_i mode. These studies show that the effect is stabilizing but becomes significant when β approaches the β_c, where β_c is the threshold β value for the ideal ballooning instability. Thus, for most discharges with $\beta \ll \beta_c$ the effect is expected to be small. However, it was also shown[15] that when the kinetic effect from the magnetic curvature drift resonance is included, the kinetic threshold value β_c^{K} becomes appreciably smaller than the usual magnetohydrodynamic (MHD) value β_c^{MHD}. This decrease of the critical β_c has two important meanings. One is that the electromagnetic ballooning mode can be kinetically unstable at the smaller β value. However, this is not expected to be a serious problem since the detailed study shows that for $\beta_c^{\mathrm{K}} \leq \beta < \beta_c^{\mathrm{MHD}}$ the real frequency of the unstable mode is much higher than the small growth rate,[15] and thus the mode will give a negligible transport effect. The second consequence of the smaller threshold β is that the electromagnetic effect can give a more significant stabilization to the toroidal η_i mode in a smaller β regime than previously considered.

Motivated by this idea we have recently developed a numerical code for solving the gyrokinetic equation in the ballooning space with the electromagnetic effect. Compared with previous approximate works, our work includes the full kinetic effects such as the magnetic curvature and parallel ion transit drift resonances as well as the finite ion Larmor radius effect. In this work, we apply the numerical code to the two TFTR supershot discharges to see how much the electromagnetic effect works in the actual system. More detailed numerical

results and comparisons with previous works of the electromagnetic effect will be given in a separated paper.[16]

Before we give the numerical results, it may be useful to consider the simple local kinetic limit to obtain some physical understanding of the electromagnetic effect. In the local kinetic limit, we will take $k_{||}$ as a variable and show that the electromagnetic effect depends significantly on the magnitude of $k_{||}$. The electromagnetic responses of the electron and ion distribution functions are given from the gyro-kinetic equation as

$$f_j = -\frac{q_j F_{Mj}}{T_j}\left[\phi - \frac{\omega-\omega^T_{*j}}{\omega-\omega_{Dj}-k_{||}v_{||}} J_0^2\left(\frac{k_\perp v_\perp}{\omega_{cj}}\right)\left(\phi - \frac{v_{||}}{c}A_{||}\right)\right] , \qquad (j=i,e) \qquad (2)$$

where $\omega^T_{*j} = \omega_{*j}[1+\eta_j(\frac{v^2}{2v_{tj}^2}-\frac{3}{2})]$, $\omega_{Dj} = \epsilon_n\omega_{*j}(\frac{v_\perp^2}{2}+v_{||}^2)/v_{tj}^2$ is the magnetic curvature drift frequency, $\omega_{*j} = -k_y cT_j/q_jBL_n$ is the electron diamagnetic drift frequency, $\eta_j = \partial \ln T_j(r)/\partial lnN(r)$, $k_{||}$ and $k_\perp$ are the parallel and perpendicular wavenumber with $k_\perp^2 = k_x^2+k_y^2$, $\epsilon_n = L_n/R$ with $L_n = -(\partial \ln N/\partial r)^{-1}$, $v_{tj} = (T_j/m_j)^{1/2}$, $\omega_{cj} = q_jB/m_jc$, and J_0 is the zeroth order Bessel function. The variables ϕ and $A_{||}$ are the perturbed electrostatic and parallel vector potential, respectively. The perpendicular vector potential $\mathbf{A}_\perp$ representing the parallel magnetic compression may be neglected for the present finite but low $\beta \ll 1$ plasma.

Now, from the quasineutrality condition

$$n_i = n_e \qquad \text{or} \qquad \int f_i d^3v = \int f_e d^3v \ , \qquad (3)$$

and the parallel Ampere's law,

$$\nabla_\perp^2 A_{||} = -k_\perp^2 A_{||} = -\frac{4\pi}{c}J_{||} = \frac{4\pi e}{c}\left(\int v_{||e} f_e d^3v - \int v_{||i} f_i d^3\right) , \qquad (4)$$

we obtain the following two basic equations in the dimensionless form,

$$\omega(1+\tau-P_0)\phi = (\tau(\omega-\omega_{*e})-k_{||}P_1)\psi \ , \qquad (5)$$

$$\frac{2k_{||}^2k_\perp^2}{\beta_i}\psi = \omega[k_{||}P_1-\tau(\omega-\omega_{*e})]\phi - [k_{||}^2P_2-\tau(\omega(\omega-\omega_{*e})-\omega_{De}(\omega-\omega_{*pe}))]\psi \ , \qquad (6)$$

where

$$P_m = \int (v_\parallel)^m \frac{\omega - \omega_{*i}\left(1+\eta_i\left(\frac{v^2}{2}-\frac{3}{2}\right)\right)}{\omega - \epsilon_n\omega_{*i}\left(\frac{v_\perp^2}{2}+v_\parallel^2\right) - k_\parallel v_\parallel} J_0^2(k_\perp v_\perp) e^{-\frac{v^2}{2}} v_\perp dv_\perp \frac{dv_\parallel}{\sqrt{2\pi}} , \qquad (7)$$

and $\tau = T_i/T_e$, $\beta_i = 8\pi N T_i/B^2$, $\omega_{*e} = k_y/\tau$, $\omega_{*i} = -k_y$, $\omega_{*pe} = \omega_{*e}(1+\eta_e)$, and $\psi = \frac{\omega v_{ti}}{ck_\parallel} A_\parallel$. Here, we note that in deriving Eqs. (5) and (6), the ordering of $\omega/k_\parallel v_{te}$, $\omega_{De}/k_\parallel v_{te} \ll 1$ has been used to take the first order terms only in the electron response. On the other hand, we have normalized the wave numbers $k_\perp$ and $k_\parallel$ to $\rho_i = v_{ti}/\omega_{ci}$ and L_n, respectively, and the frequencies ω and ω_* to v_{ti}/L_n.

To better understand the physical contents of Eqs. (5) and (6) we briefly consider the well-known fluid limit of $|\omega_D/\omega| \ll 1$, $|k_\parallel v_e/\omega| \ll 1$ and $k_\perp^2 \ll 1$. In this limit, Eq. (7) gives

$$P_0 \simeq 1 - \frac{\omega_{*i}}{\omega} + \left(\frac{\omega_{Di}}{\omega} - k_\perp^2 + \frac{k_\parallel^2}{\omega^2}\right)\left(1 - \frac{\omega_{*pi}}{\omega}\right) ,$$

$$P_1 \simeq \frac{k_\parallel}{\omega}\left(1 - \frac{\omega_{*pi}}{\omega}\right) , \qquad P_2 \simeq 1 - \frac{\omega_{*pi}}{\omega} ,$$

with $\omega_{*pi} = \omega_{*i}(1+\eta_i)$ and $\omega_{Di} = 2\varepsilon_n\omega_{*i}$, so that Eqs. (5) and (6) reduce to, respectively,

$$\left[\tau\left(1 - \frac{\omega_{*e}}{\omega}\right) - \frac{k_\parallel^2}{\omega^2}\left(1 - \frac{\omega_{*pi}}{\omega}\right)\right](\phi - \psi) + \left(k_\perp^2 - \frac{\omega_{Di}}{\omega}\right)\left(1 - \frac{\omega_{*pi}}{\omega}\right)\phi = 0 , \qquad (8)$$

$$\omega(\omega - \omega_{*pi})k_\perp^2\phi = \frac{2k_\parallel^2 k_\perp^2}{\beta_i}\psi + \omega_{Di}(\omega - \omega_{*pi})\phi + \tau\omega_{De}(\omega - \omega_{*pe})\psi , \qquad (9)$$

We note that Eqs. (8) and (9) are the continuity and vorticity equations, respectively, in the incompressible fluid limit. Equations (5)–(6) or (8)–(9) describe the coupling of the electrostatic drift wave and the electromagnetic shear Alfvén wave. In the electrostatic limit of $\beta_i \to 0$, Eq. (9) gives $\psi = 0$, and then Eq. (8) reduces to the electrostatic η_i mode equation in the local fluid limit. On the other hand, in the shear Alfvén limit where $\omega \simeq \omega_{*pi}$, Eq. (8) gives $\phi = \psi$, and Eq. (9) becomes the ideal ballooning mode equation in the local fluid limit. In this limit, it is easy to see that the ideal ballooning instability is generated when $\beta \geq \beta_c \sim k_\parallel^2/\varepsilon_n[1 + \eta_i + (1+\eta_e)/\tau)]$. Here, we note that the ballooning stability threshold value β_c is a sensitive function of $k_\parallel$. This suggests that the electromagnetic effect also will

depend significantly on $k_{||}$. Thus, we first consider the $k_{||}$ dependence of the toroidal η_i mode using the local kinetic equations (5) and (6), even though the $k_{||}$ is an operator in the nonlocal case.

Figure 2 shows the normalized growth rate as a function of $k_{||}$ for various β_i values when $\eta_i = 2.5, \eta_e = 2.1$, $\varepsilon_n = 0.18$, $T_i/T_e = 1.5$ and $k_y\rho_i = 0.5$, which correspond to the parameter set at $r = 0.3$m of discharge 44669 A. In Fig. 2 we note that the solid curve corresponds to the toroidal η_i mode, while the dashed line represents the the kinetic-MHD ballooning mode, which is destabilized very rapidly with the decreasing $k_{||}$. Figure 2 shows that the electromagnetic effect gives an overall stabilizing effect on the toroidal η_i mode in agreement with previous results. In particular, for a given finite β_i the stabilizing effect becomes strong as $k_{||}$ decreases, that is, the threshold value $\beta_c(\propto k_{||}^2) \rightarrow \beta_i$. When $k_{||}$ approaches to $k_{||,\mathrm{crit}}$ where $\beta_i \simeq \beta_c$, the growth rate of the toroidal η_i mode becomes zero and the kinetic-MHD ballooning mode is destabilized. Thus, Fig. 2 shows that, in terms of a local $k_{||}$ approximation, the toroidal η_i mode is almost completely stabilized by the coupling with the shear Alfvén wave at the region $k_{||} \leq k_{||,\mathrm{crit}}$ or equivalently $\beta \geq \beta_c$.

These local results now suggest that in the electromagnetic regime of finite $\beta_i(> 10^{-3})$ the unstable toroidal η_i modes should try to maximize $k_{||}$ to reduce the stabilizing coupling with the shear Alfvén wave. However, the increasing $k_{||}$ also means the increase of the stabilizing effect of the parallel ion transit drift term $k_{||}\, v_{ti}$. Thus, there is an optimum $k_{||}$ value (denoted by $k_{||,\mathrm{max}}$), where the growth rate becomes maximum, for example at $\beta_i = 0.006$ the $k_{||,\mathrm{max}} L_n \simeq 0.12$ in Fig. 2. Comparing this maximum growth rate with that in the electrostatic limit, we find that it has been significantly reduced (at $\beta_i = 0.006$ by a factor 3) by the combination of the shear Alfvén wave coupling and the parallel ion transit drift ($k_{||}\, v_{ti}$) effects.

Now, we present the results of solving the nonlocal gyrokinetic equation. Figure 3 show the maximum growth rates as a function of the minor radius for the TFTR 44669A discharge

in the electrostatic and electromagnetic regimes. The nonlocal results are also compared with the local results maximized over $k_{||}$. First, compared with the electrostatic case, we find that the electromagnetic case has much smaller maximum growth rates in the intermediate core region. Near the edge region, the electromagnetic effect is found to be negligible. On the other hand, in the electromagnetic case the more exact nonlocal value is smaller than the local value at $k_{||,\mathrm{max}}$. Also, it is worthwhile to note that our nonlocal results for the growth rate and the real frequency have been compared with those of Rewoldt[17] for the parameters of TFTR 44669A at $r = 0.3$m and found to be in good agreement for both the η_i mode and the kinetic-MHD ballooning mode.

In Fig. 4, we show the χ_i values obtained with the the electromagnetic effect for the two supershot discharges of TFTR 44669A and TFTR 51025. Now, the χ_i's are in much better agreement with the experiment in the core region. (To obtain agreement in χ_i with χ_i^{exp} in the outer half region of the plasma the mixing length formula will be modified as discussed later). Thus, we conclude that the decrease of χ_i in the core region can be mostly explained if we consider the electromagnetic effect.

Here, we show other experimental evidences that seem to support this conclusion that β_i plays an important role in the core transport. First, comparing a recent hot ion H-mode experiment[2] by Taroni *et al.* in JET with the TFTR 44669A supershot experiment, we find that TFTR has a much larger χ_i value (about 4 times on average) than JET. Since the two experiments have almost the same magnitude and profiles for T_i, T_e, n_e, while in the toroidal magnetic field TFTR is about 1.7 larger than the JET, the main difference between the two experiments is that JET has the β_i value which is about three times larger than that of TFTR. Thus, even though there can be other possibilities such as the q and geometry effects, the smaller value of the χ_i in JET may be due to the larger electromagnetic effect from the three times higher β_i. Secondly, the experiment[2] of the L to H transition in DIII-D by Burrell *et al.* shows the significant decrease of the χ_i in the core region after the L to

H transition. During the transition, there are no appreciable changes in the profiles of $T_{i,e}$ and q, while the density profile flattens more with the significant increase of the density. If we note that the flattening of the density profile does not contribute to the stabilization, in terms of the η_i mode there is no other proper explanation of the stabilization, besides that due to the electromagnetic effect by the increased density (the electrostatic dispersion relation is independent of density). Finally, a recent experiment[18] by Hirayama *et al.* in JT-60 shows that there is a significant decrease of the χ_i in the core region when the density only is increased by about two times. All these experiments suggest that the electromagnetic or density effect plays an important role in reducing the ion thermal transport in the core region.

Now, since we have obtained a plausible solution about the problem of why the χ_i decreases in the core region, we turn our attention to the second problem of why the experimental $\chi_i(r)$ increases with minor radius. As can be seen in Fig. 4 the traditional mixing length formula (based on $k_{\perp,\mathrm{max}}$) does not explain this trend. This contradiction between the simple mixing length transport and experiment suggests the following two possibilities: one is that the actual transport near the edge region is not by the ion temperature gradient mode, and the second is that the traditional mixing length formula can significantly underestimate the actual transport.

Here, we consider the second possibility and propose a new mixing length formula. We note that there are numerical simulation results[19,20] which show that the simple mixing length estimate may underestimate the actual transport. Our idea for the new formula is basically based on the inverse cascade phenomena, which was observed in numerical simulations[6] for the modeling of the nonlinear interaction of the η_i mode in the slab limit. As shown there, in the turbulent state the energy of the short wavelength modes cascade to the long wavelength side, making the most long wavelength mode dominate the fluctuation energy. This inverse cascade suggests that the dominant radial mode width in the turbulent state will be closer to

the longest wavelength mode still unstable, rather than that of the fastest growing mode as assumed in the traditional mixing length formula. A recent fluctuation study by Mazzucato[21] also supports this feature since the correlation length measured by the reflectrometer seems to be much larger than the $1/k_{y,\max}$. Thus, if we take the radial mode width as $k_{y,\min}$ and still assume that the saturation level of the fluctuation is proportional to the maximum growth rate $\gamma_{\max}$, we are lead to the following new mixing length formula

$$\chi_i = \frac{\gamma_{\max}}{k_{y,\min}^2} . \tag{10}$$

If there were no damping mechanism for the long wavelength modes, the longest wavelength will be determined by finite geometry as $k_{y,\min} \simeq 1/r$ and then the formula (10) will give much higher χ_i value than the experiment. However, a strong linear damping of the long wavelength modes can take place for the toroidal η_i mode by the parallel ion transit drift effect.

To explain briefly this stabilization of the long wavelength mode, we consider the gyrokinetic equation of the local form, $(\omega-\omega_D-k_{\|}v_{\|})h = \frac{q}{T}(\omega-\omega_*^T)J_0F_M\phi$, where h is the nonadiabatic part of the perturbed distribution function. From this form of the gyrokinetic equation, we can see that the parallel ion transit drift dominate the curvature drift if $k_{\|}v_{\|} > \omega_D$. As shown more explicitly in Ref. 9, this condition actually corresponds to the mode transition condition from the toroidal to the slab η_i mode. Thus, the toroidal mode can be considered as stabilized when the condition is satisfied. Here, if we use the usual local approximation $\omega_D = \omega_D(\theta = 0) = 2\varepsilon_n\omega_{*i}$ the above condition becomes $k_y\rho_i < k_{\|}R/2$. From this simple form, we can see that the long wavelength toroidal η_i modes with $k_y\rho_i \leq (k_y\rho_i)_{\min} \sim k_{\|}R/2$ are linearly stabilized.

Here, we note that the value of $k_{\|}$ is linked to the value $(k_y\rho_i)_{\min}$. In the electrostatic limit, the nonlocal analysis showed $k_{\|} \sim 1/2Rq$. On the other hand, in the electromagnetic regime, $k_{\|}$ must increase to reduce the stabilizing coupling with the shear Alfven wave and

we may approximate $k_{||} \simeq k_{||,\max}$. Here, $k_{||,\max}$ depends significantly on the β_i value and increases with β_i along the approximate formula $k_{||,\max} \propto \sqrt{\beta_i}$, as shown in Fig. 2. We can estimate from Fig. 2 that for $\beta_i = 0.0045$, which is the β_i value at $r = 0.3$m of the discharge TFTR 44669A, the $k_{||,\max} L_n$ value is about 0.11, and which closely corresponds to $k_{||} \simeq 1/Rq$ for this radius. The mode with $k_{||} \simeq 1/2Rq$ (or $k_{||} L_n \simeq 0.06$), which corresponds to the electrostatic mode at $\beta_i = 0$, is almost stabilized by the strong coupling with the shear Alfven wave at this β_i value. Thus, even though it is not easy to determine the $k_{||}$ value exactly, it seems possible to take $k_{||} \sim 1/Rq$ as the first approximation for the dominant $k_{||}$.

Here, we consider the implication of taking the value $k_{||} \sim 1/Rq$ as the first approximation. Then, the above stabilization condition of the long wavelength toroidal η_i mode gives $(k_y \rho_i)_{\min} \sim 1/2q$. Thus, our new formula Eq. (10) becomes

$$\chi_i \simeq 4\gamma_{\max} \rho_i^2 q^2 \ , \tag{11}$$

where $\gamma_{\max}$ is a numerically determined function of the tokamak parameters. We note that compared with the usual mixing length formula (1), the new formula (11) has a additional strong q dependence. This strong q dependence gives the χ_i, which is q^2 times larger than the previous formula (1).

In Fig. 4(a), we show the χ_i calculated by this new formula for the discharge TFTR 44669A. We find that the new χ_i agrees well with the experiment over most of the minor radius. A similar agreement is also found for the another TFTR supershot discharge (shot number 51025), as shown in Fig. 4(b). Thus, we find that by the strong q dependence the new formula can well explain the observed radial increase of the χ_i. On the other hand, we note that the q dependence[8,22] is a crucial factor which most previous theoretical models of the η_i transport have failed to produce, while the experimental scaling law both in the Ohmic heated[23] and auxiliary heated[24] plasmas require such a dependence. Our new formula provides a plausible solution of the physical origin of such q dependence. Noting

that $\rho_i^2 = m_i T_i / e^2 B^2$ and $q = rB/RB_\theta$, it is easy to see that the new formula has a very weak B dependence, and a favorable current scaling of $\chi_i \propto 1/I^2$ (Of course, here, it should be noted that some additional dependences on B and I can come through the $\gamma_{\max}$). These dependences do not agree exactly with the empirical scaling law, but they are in much better agreement than the conventional simple mixing length formula.

Here, it may be useful to note a recent experimental result by Zarnstorff *et al.* which investigates how the χ_i varies when the q profile is changed. This current ramp experiment has produced the somewhat surprising result that the χ_i does not follow directly the change of q. From this result Zarnstorff *et al.*[2] suggest that the strong q dependence may come from the inner region, or the nonlocal dependence on the current profile. Here, we try to explain this behaviour by our model. First, we note that the sudden increase of q by the decrease of the current will decrease significantly $k_\parallel^2$ ($\propto 1/q^2$) term, making β_c ($\propto k_\parallel^2$) approach β_i. As discussed earlier, this means the significant increase of the electromagnetic effect, and thus the substantial reduction of the growth rate of the toroidal η_i mode. Thus, the increase of the radial mode width, which is proportional to $k_{y,\min}^{-1} \sim 2q\rho_i$ in our model, will be compensated by the decrease of the the maximum growth rate, making the χ_i almost unchanged. The increase of the χ_i after some time may be caused by the increase of the growth rate which occurs since the electromagnetic effect will be reduced by the ongoing radial anomalous transport. Thus, our model suggests that the effect of q is closely related with the electromagnetic effect.

In this work, we have not considered the effect of trapped particles, for simplicity. One particular feature of the trapped particles is that they are less sensitive to the stabilizing effects of the parallel transit drift. Thus, the trapped particles are expected to give some more destabilizing effect, as shown in some recent works.[25,26] We also note that the trapped ion mode can be generated in the very low frequency and longer wavelength regime.

Summarizing, we have shown that it is possible to explain some of important properties

of the observed χ_i using the toroidal η_i mode turbulence model. First, we have shown that the observed reduction of $\chi_i(r)$ in the core region can be explained by the electromagnetic effect. Secondly, we have proposed a new mixing length formula which can well explain the radial increase of the $\chi_i(r)$ and gives the scaling law in the current and magnetic field which agrees well with the experiment. Our new formula of the ion thermal transport would be important for analyzing other hot ion mode discharges. Finally, we note that our new formula is based on two essential assumptions: (1) the inverse cascade to the long wavelength side, and (2) the strong linear damping of the long wavelength toroidal η_i mode by the parallel ion transit drift term (in particular, note the formula (11) bases on the choice $k_{\|} = 1/Rq$). It will be important to check these by more advanced analytical and numerical methods. In particular, the electromagnetic gyrokinetic simulation in the toroidal geometry, which is a main goal of the recent Numerical Tokamak Project, is expected to provide a reliable test.

Acknowledgments

The authors would like to thank J.Q. Dong for helping the numerical work. They also thank S.D. Scott, G.W. Hammett, M.C. Zarnstorff, and other TFTR experimental team for useful discussions and for providing the discharge data.

This work is supported by the U.S. Department of Energy under contract #DE-FG05-80ET-53088.

References

1. S.D. Scott *et al.* Phys. Rev. Lett. **64**, 531 (1990); S.D. Scott *et al.* Phys. Fluids B **2**, 1300 (1990).

2. M.C. Zarnstorff *et al.* in *Plasma Physics and Controlled Nuclear Fusion Research*, 1990, Proceedings of the 12th International Conference, Washington (IAEA, Vienna, 1991), Vol. I, p. 109; A. Taroni *et al. ibid*, Vol. I, p. 93; K.H. Burrell *et al. ibid*, Vol. 1, p. 123.

3. F. Romanelli, Phys. Fluids B **1**, 1018 (1989).

4. R.R. Dominguez and M.N. Rosenbluth, Nucl. Fusion **29**, 844 (1989).

5. W. Horton *et al.* Phys. Fluids B **4**, 953 (1992).

6. S. Hamaguchi and W. Horton, Phys. Fluids B **2**, 1833 (1990) and *ibid* 3040(1990).

7. M. Kotschenreuther *et al.* in *Plasma Physics and Controlled Nuclear Fusion Research*, 1990, Proceedings of the 12th International Conference, Washington (IAEA, Vienna, 1991), Vol. II, p. 361.

8. R.E. Waltz, Phys. Fluids **31**, 1962 (1988).

9. J.Y. Kim and W. Horton, Phys. Fluids B **3**, 1167 (1991).

10. J.Q. Dong, W. Horton, and J.Y. Kim, to be published in Phys. Fluids, July (1992).

11. T.S. Hahm and W.M. Tang, Phys. Fluids B **1**, 1185 (1989).

12. W. Horton, J.E. Sedlak, D.I. Choi, and B.G. Hong, Phys. Fluids **28**, 3050 (1985).

13. R.R. Dominguez and R.W. Moore, Nucl. Fusion **26**, 85 (1986).

14. A. Jarmen, P. Anderson, and J. Weiland, Nucl. Fusion **27**, 841 (1987).

15. B.G. Hong, W. Horton, and D.-I. Choi, Plasma Phys. Controlled Fusion **31**, 1291 (1989); B.G. Hong, W. Horton, and D.-I. Choi, Phys. Fluids B **1**, 1589 (1989).

16. J.Y. Kim and W. Horton, *"The electromagnetic effect on the toroidal η_i mode"*, to be submitted to the Plasma Phys. and Controlled Fusion.

17. G. Rewoldt, W.M. Tang, and M.S. Chance, Phys. Fluids **25**, 480 (1982), and private communication.

18. T. Hirayama, H. Shirai, M. Yagi, K. Shimizu, Y. Koide, M. Kikuchi, and M. Azumi, Nucl. Fusion **32**, 89 (1992).

19. G.S. Lee and P.H. Diamond, Phys. Fluids **30**, 3291 (1986).

20. B.A. Carreras, L. Garcia, and P.H. Diamond, Phys. Fluids **30**, 1388 (1987).

21. E. Mazzucato, private communication.

22. R.E. Waltz, R.R. Dominguez, and F.W. Perkins, Nucl. Fusion **29**, 351 (1989).

23. W. Horton, R.D. Estes, Nucl. Fusion **19**, 3 (1979)

24. S.M. Kaye, Phys. Fluids **28**, 2327 (1985).

25. G. Rewoldt and W.M. Tang, Phys. Fluids B **2**, 318 (1990).

26. J. Weiland and A. Hirose, Nucl. Fusion **32**, 151 (1992).

Figure Caption

1. Comparison of three theoretical models of ion thermal conductivity with experimental result for the TFTR 44669A supershot discharge in the electrostatic limit.

2. The normalized growth rate as a function of $k_{\parallel}$ for various β_i values when $\eta_i = 2.47$, $\eta_e = 2.1$, $\varepsilon_n = 0.18$, $T_i/T_e = 1.5$, and $k_y\rho_i = 0.5$.

3. The maximum growth rate as a function of minor radius in the electrostatic (nonlocal) and electromagnetic (local and nonlocal) cases for the TFTR 44669A supershot discharge.

4. Comparison of two theoretical models of ion thermal conductivity with experimental result in the electromagnetic regime (a) for the TFTR 44669A supershot discharge, (b) for the TFTR 51025 supershot discharge.

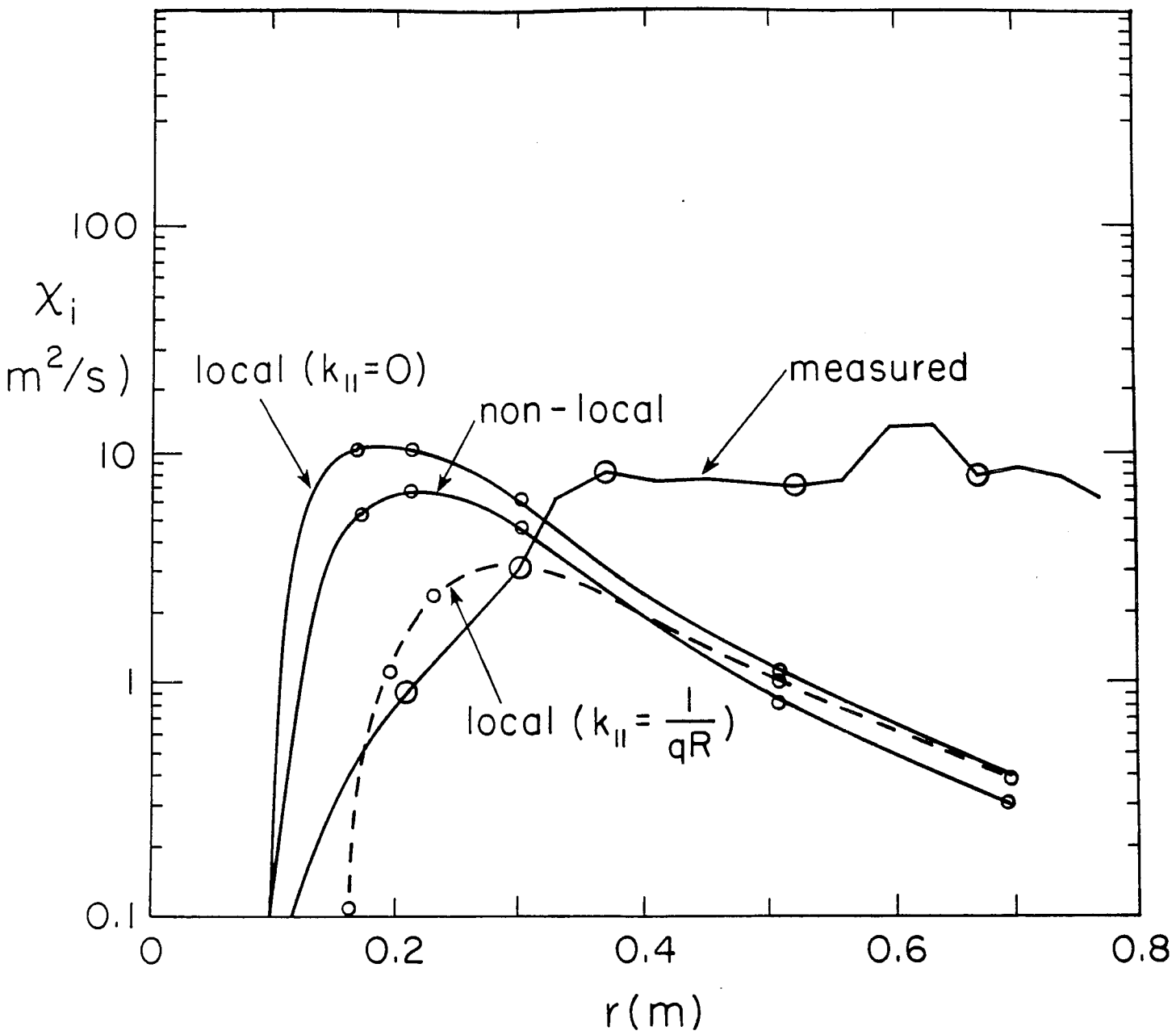
100
10
1
0.1
χ_i
m^2/s)
local ($k_{||}$=0)
non-local
measured
local ($k_{||} = \frac{1}{qR}$)
0
0.2
0.4
0.6
0.8
r(m)

Fig. 1

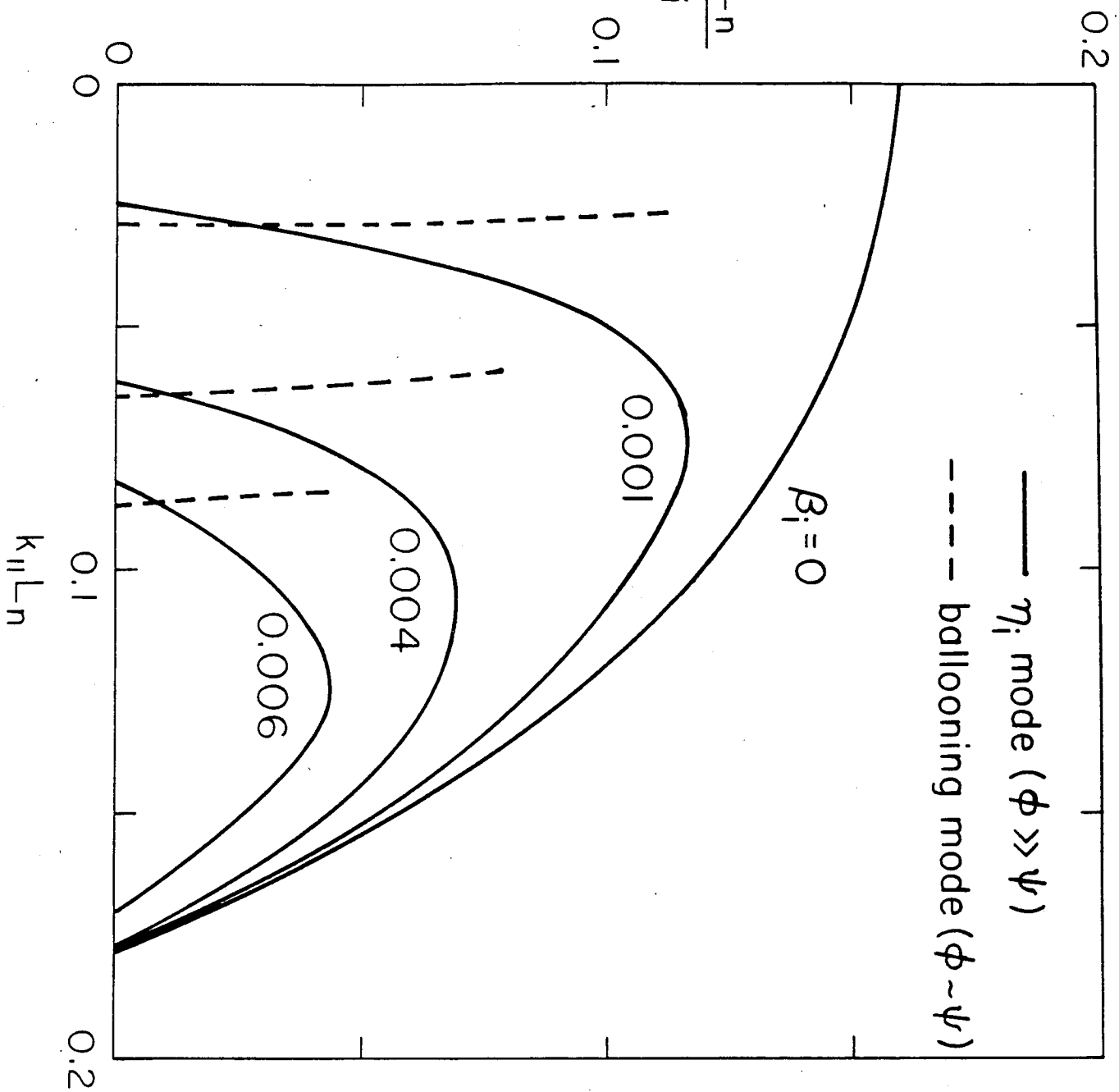
0.2
0.1
0
0
0.1
0.2
$\frac{\gamma L_n}{v_i}$
$k_{\parallel} L_n$
η_i mode ($\phi \gg \psi$)
ballooning mode ($\phi \sim \psi$)
$\beta_i = 0$
0.001
0.004
0.006

Fig. 2

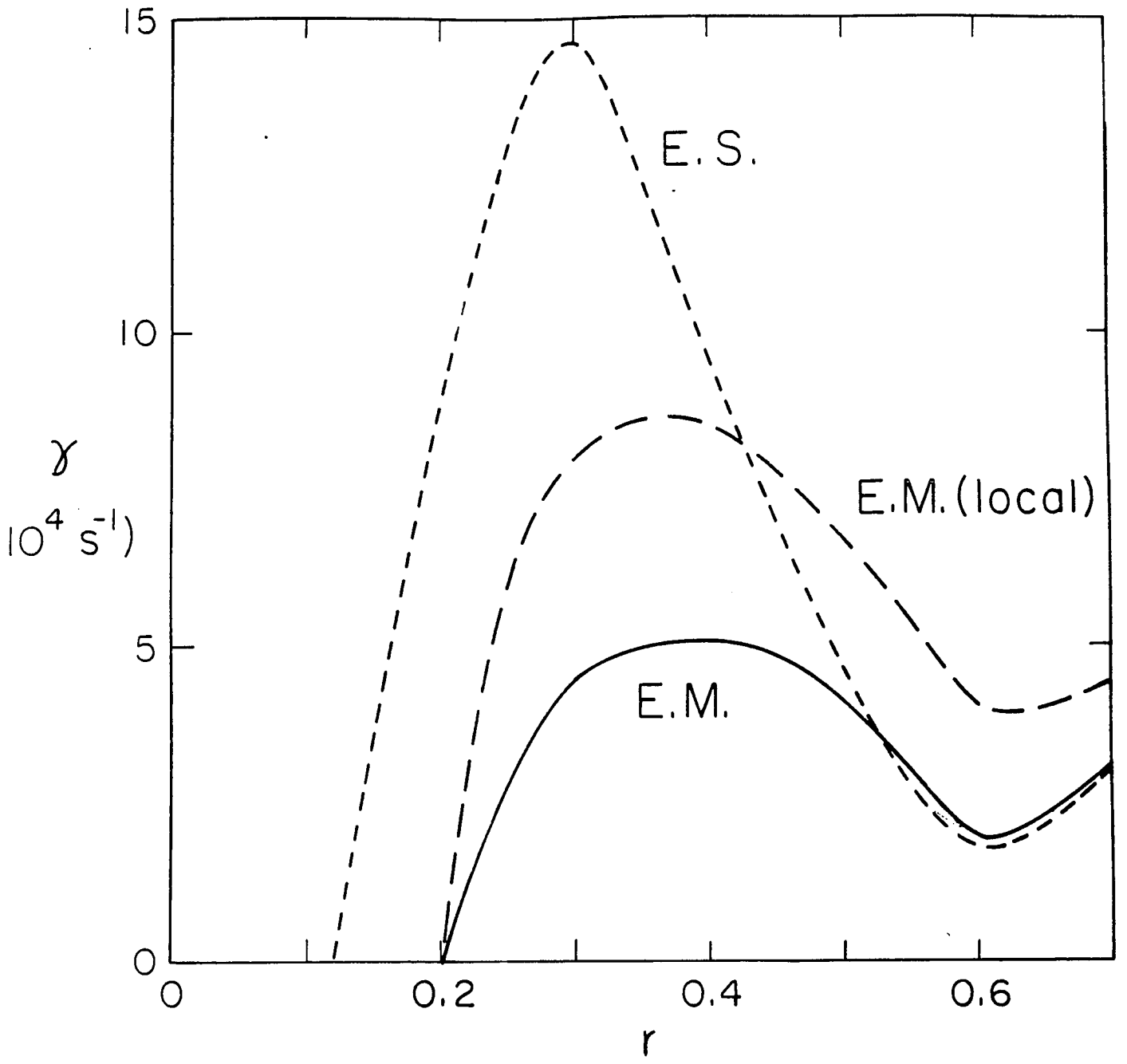

Fig. 3

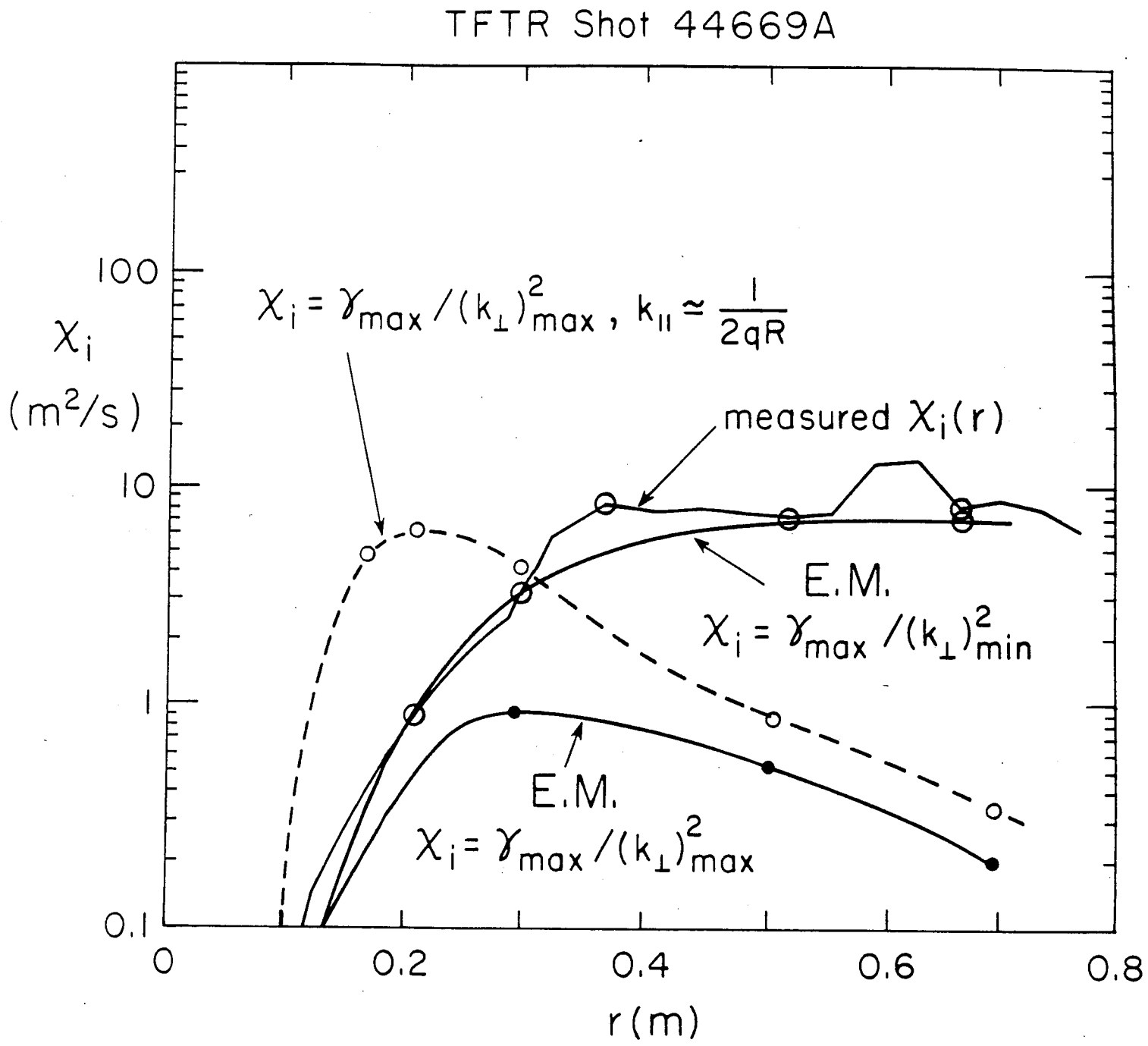
TFTR Shot 44669A
100
10
1
0.1
χ_i
(m^2/s)
$\chi_i = \gamma_{max}/(k_\perp)^2_{max}$, $k_{11} \simeq \frac{1}{2qR}$
measured $\chi_i(r)$
E.M.
$\chi_i = \gamma_{max}/(k_\perp)^2_{min}$
E.M.
$\chi_i = \gamma_{max}/(k_\perp)^2_{max}$
0
0.2
0.4
0.6
0.8
r(m)

Fig. 4(a)

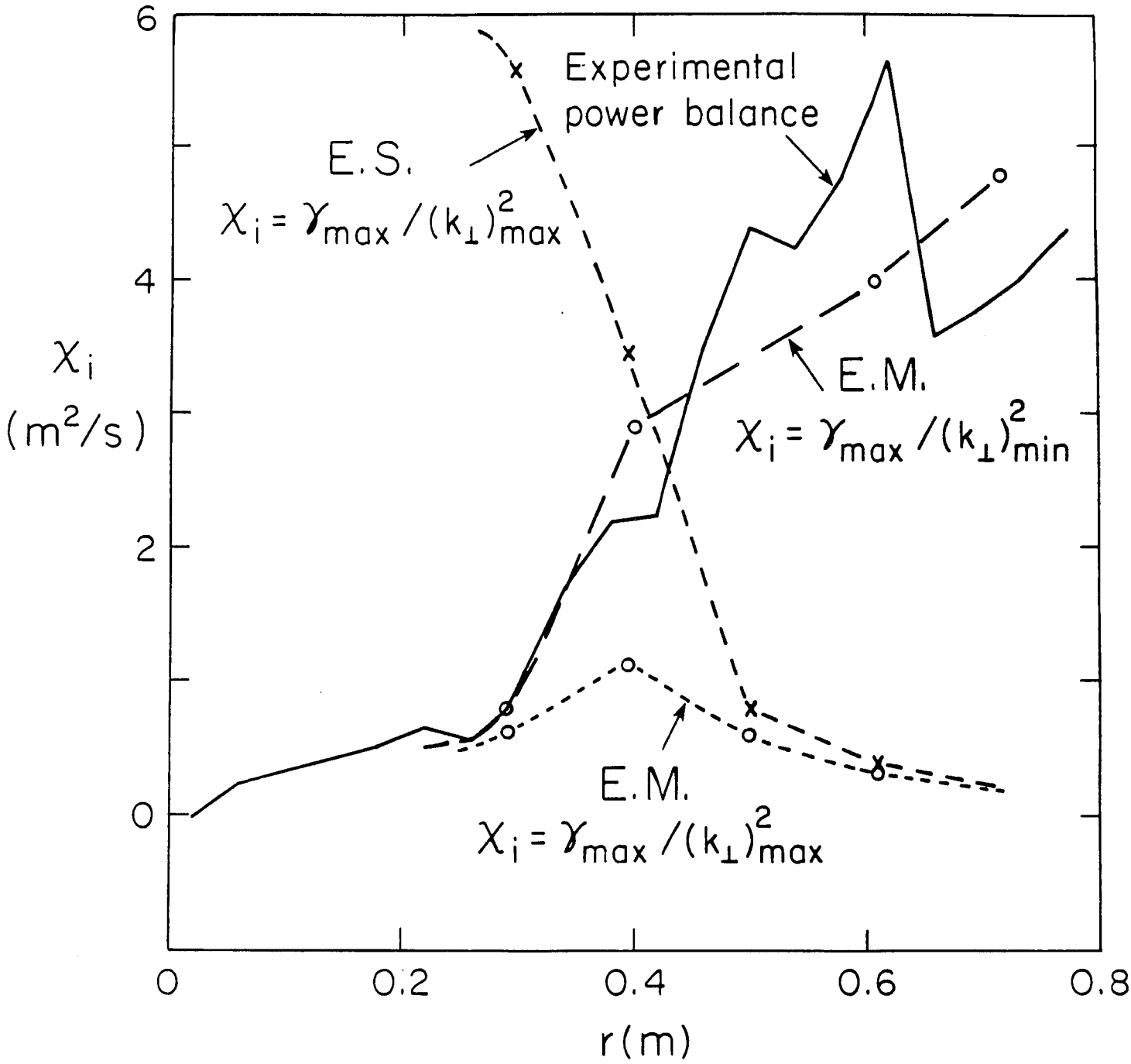
6
4
2
0
χ_i
(m^2/s)
Experimental
power balance
E.S.
$\chi_i = \gamma_{max} / (k_\perp)^2_{max}$
E.M.
$\chi_i = \gamma_{max} / (k_\perp)^2_{min}$
E.M.
$\chi_i = \gamma_{max} / (k_\perp)^2_{max}$
0
0.2
0.4
0.6
0.8
r(m)

Fig. 4(b)